JOURNAL OF MECHANICS OF CONTINUA AND MATHEMATICAL SCIENCES
www.journalimcms.org

ISSN (Online) : 2454 -7190 Vol.-19, No.-11, November (2024) pp 79-97 ISSN (Print) 0973-8975

NETWORK FUNCTION VIRTUALIZATION FOR UNDERWATER ACOUSTIC WIRELESS COMMUNICATION USING STOCHASTIC NETWORK CALCULUS

T. C. Subash Ponraj[1], Rajeev Sukumaran[2]

[1, 2] Computer Science and Engineering, SRM Institute of Science and Technology, Kattankulathur, Chengalpattu, Tamil Nadu 603203 India.

[1]subashponraj2@gmail.com, [2]rajeevcbe@gmail.com

Corresponding Author: **T. C. Subash Ponraj**

https://doi.org/10.26782/jmcms.2020.11.00006

(Received: August 20, 2024; Revised: October 22, 2024; Accepted: November 05, 2024)

Abstract

Wireless communication in marine environments is hindered by the unique properties of seawater and the rugged ocean floor. In contrast to land-based communication, underwater conditions are distinct due to the specific characteristics of seawater. This research explores the potential of Network Function Virtualization (NFV) to enhance the monitoring of seaweed farms and underwater properties. As seaweed production is vital for the development of nutritional products, biochemical compounds, and pharmacological research, optimizing its monitoring is crucial. The goal of this study is to leverage NFV to support various aquatic activities. To achieve this, a chain of Virtual Network Functions (VNFs) is proposed to manage service flows, capitalizing on the advancements in NFV. The research employs both simulation and analytical Stochastic Network Calculus (SNC) models to evaluate key performance indicators, including delay bounds, throughput, packet delivery ratio, and energy utilization. Notably, the SNC-based NFV model outperforms simulation results, demonstrating superior performance and potential for improved packet delivery and throughput.

Keywords: Underwater acoustic wireless communication; Network Function Virtualization; Stochastic Network Calculus; Delay bound

I. Introduction

Underwater Wireless Sensor Networks (UWSNs) have garnered significant attention from researchers due to their versatility and capabilities. They play a vital role in various applications, including disaster prevention, military defense strategies, pollution tracking, and environmental and underwater resource monitoring. Underwater sensor nodes collect and transmit data to a buoy, providing real-time insights into underwater environments. UWSNs have revolutionized our

understanding and interaction with aquatic ecosystems [V]. However, despite the growing demand for UWSNs, there are still significant limitations on network performance and the capabilities of sensor nodes in the monitored region. Although a wide range of application requirements have been presented, underwater sensor nodes are constrained by their limited capacity and power, as well as the complexity of reliable communication paths and acoustic signal transmission [XXV]. The integration of seaweed farming into aquaculture has been shown to have numerous benefits. For example, seaweed farming can create a healthier environment for shrimp, fish, and shellfish farms by producing oxygen through photosynthesis, thereby promoting healthy growth.

Underwater meadows are vital ecosystems that support a diverse range of marine life, including herbivores like dugongs, green sea turtles, and certain fish species. These seaweed beds also contribute to improved water quality by filtering pollutants and providing a safe haven for young marine organisms. A promising innovation in seaweed farming is the use of sensor-based data collection. This technology enables efficient monitoring of the underwater environment, including seaweed growth, sunlight availability, and water quality predictions. Network Function Virtualization (NFV) is revolutionizing network operations by allowing operators to move away from specialized hardware for each network function. Instead, NFV enables the creation of service flows using Virtual Network Functions (VNFs) that run on standard servers. This approach transforms network functions, such as firewalls, into professional-grade services [XIX]. By leveraging NFV, network operators can decouple network functions from dedicated hardware [XXVIII]. This means that a firewall, for example, can be deployed as a VNF on standard servers, offering greater flexibility and efficiency.

Software Defined Networking (SDN) [XVII], [XII] facilitates the powerful redirection of traffic among VNFs, enabling the sequential connection of VNFs to deliver various services. This paper aims to establish the maximum delay limits for a series of VNFs, specifically known as a Service Function Chain (SFC). Many existing works [IV], [XXI] have assumed that the delay experienced by flows moving via VNFs remains constant. However, to calculate the end-to-end delay experienced by an SFC, this approach sums the delays introduced by both the links and the VNFs in the chain, which leads to notable inaccuracies since the processing delay of VNFs can vary depending on the allocated resources. The adoption of Network Calculus to determine the delay of an SFC has produced a reliable and delay-bound analysis in terrestrial networks [XXVI]. While some studies [III], [X] apply queuing theory to determine SFC delay, the average delay may not guarantee timely packet delivery in worst-case scenarios, as this approach may not ensure timely delivery under all conditions. To address these challenges, specific studies employ Network Calculus to set delay bounds for Service Function Chains. The pioneering application of Network Calculus [VII] for analyzing a single flow within SFCs has provided valuable insights through formula derivation. Miao et al. [XVIII] introduced a stochastic Network Calculus model to analyze end-to-end performance limits in shared infrastructures, addressing resource competition but not exploring Service Function Chains with priority queues. Further research is necessary to understand the impact of priority queues on network performance in such scenarios.

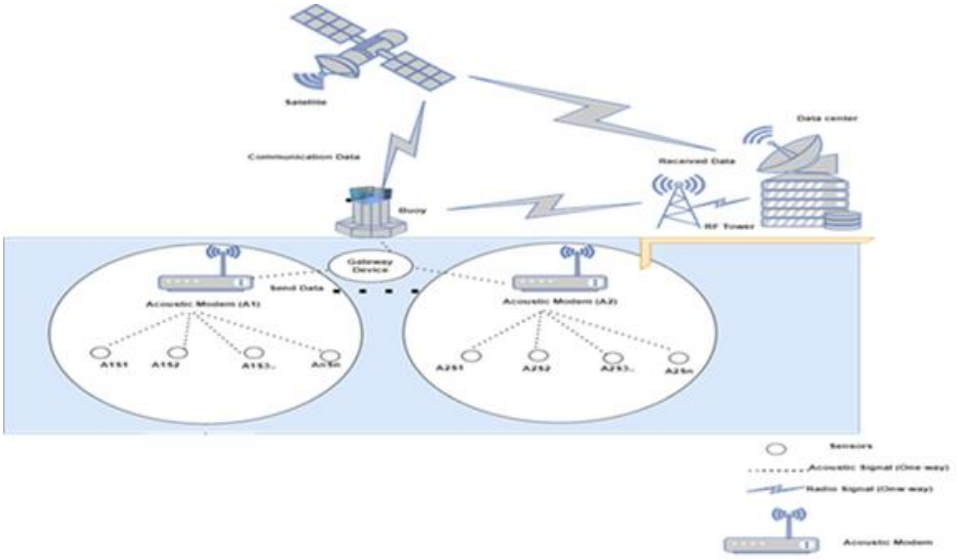

Fig. 1. Architecture of UWSN

This research explores a scenario where flows utilize VNF instances with per-VNF priority. The study investigates methods to analyze delays in service chains, considering the adjustable resource usage of VNFs and predicting data arrival rates using Token Bucket Filters (TBFs). SNC [XXII] is applied to calculate maximum delays in service chains. The proposed system is used to verify the accuracy of these methods. **Fig 1** illustrates the architecture of the Underwater Wireless Sensor Networks. In this system, sensor nodes collect data from the underwater environment and transmit it using acoustic modems. The buoy receives various types of data, including seaweed height, temperature, water quality, and sediment type, and sends this information to the data center through communication signals.

Section II provides a review of related works in the field of underwater research. Section III presents a detailed analysis of delays in an underwater environment using SNC. Section IV describes the implementation process using a simulation model. Section V concludes the study and discusses potential avenues for future research.

II. Literature Review

While deterministic approaches have been used to analyze network performance in underwater fish farming, SNC models have not yet considered frame flow control methods [XVI]. The proposed model aims to address this gap by applying SNC to analyze performance in underwater communication systems. This section explores existing simulation models for Transport layer protocols in Underwater Wireless Sensor Networks (UWSNs). The Transmission Control Protocol (TCP) is generally not well-suited for UWSNs due to its reliance on reliable connections and inefficiency in limited bandwidth environments [II]. Underwater communication challenges, such as significant delays and high packet loss rates, further exacerbate TCP's shortcomings. The U-New Reno protocol, a modified version of TCP, has been developed to address these challenges in UWSNs [XI]. While U-New Reno offers

improvements for underwater transmissions, the article does not explicitly discuss its energy efficiency for packet delivery.

Routing protocols in underwater sensor networks act as navigators, guiding data from sensor nodes to a central collection point on the surface. These protocols must find efficient routes that minimize energy consumption while ensuring reliable data delivery [XIII, XIV]. However, the provided description lacks a specific timeframe for data packet delivery. Underwater sensor data often contains high redundancy, but traditional data compression techniques may not be effective due to limitations in underwater communication [I, VIII]. Additionally, data loss is a potential limitation for certain data transfer algorithms, impacting their ability to ensure complete and accurate data delivery [XXVII]. Applications built on the Transmission Control Protocol (TCP) prioritize reliable, in-order data delivery, which is crucial for ensuring the correct transmission of important information. However, this can result in slow data transfer in underwater environments due to the limitations of the medium. Consequently, TCP is not ideal for underwater sensor networks.

III. Modeling and Analyzing Delay Underwater Seaweed Farm with Stochastic Network Calculus

This section explores the system model for VNF and the importance of SNC SNC-based model to analyze the delay bound, backlogs, throughput, and Packet Delivery Ratio (PDR).

VNF system model for Underwater Environment

This model aims to determine the guaranteed wait time (delay bound) for data flows passing through a series of VNFs. Each VNF utilizes two priority queues—high and low—to effectively manage data traffic. Our model accommodates multiple priority queues and assigns per-VNF priorities to service flows, enhancing network performance and efficiency. **Fig 2** depicts a system model with J VNFs. In this model, user flows are shaped by TBFs and then sequentially pass through the VNFs before reaching service providers. Within each VNF, packets are received from the Acoustic Modem, classified, and routed to the appropriate queues. The packet processing mechanism ensures efficient retrieval. This comprehensive approach prioritizes data flows, optimizing network performance in underwater environments characterized by limited bandwidth and significant delays.

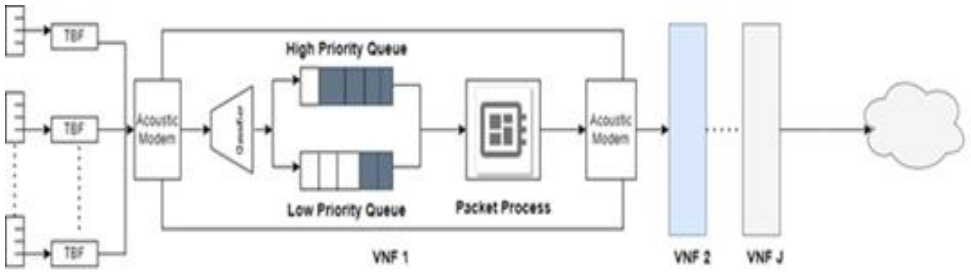

Fig. 2. System Model

NFV is particularly well-suited for the Network and Transport layers of underwater communication networks The Network layer, optimal data packet routing is crucial.

The Geographic Adaptive Routing (GAR) protocol is ideal for routing data in underwater environments due to its focus on location awareness and energy efficiency. When transmitting data, a node initiates a route discovery process to establish an efficient path. While GAR does not directly ensure data reliability, it can indirectly impact it by selecting routes that minimize packet loss, which is particularly important in underwater environments with significant signal attenuation and interference. The Transport layer, the User Datagram Protocol (UDP) works with IP to facilitate reliable data transfer between applications. UDP sends data packets, and the receiver processes them if they are received accurately. To send data to another node, a route discovery procedure must be initiated to establish an efficient path. This process is essential for ensuring reliable and efficient data transmission in underwater communication networks.

Maximum and Minimum communication bounds using SNC

This research study utilizes SNC to establish the supremum and infimum communication range. Two key concepts are employed: the arrival curve, which represents the maximum data flow that can be sent, and the service curve, which guarantees the minimum service provided by the network device [XXIII]. The data arriving at a TBF is limited by an arrival curve, mathematically expressed as $A(t) \leq \rho t + \sigma$. In this context, σ represents the token bucket size and ρ represents the token rate. The TBF can send σ bits at once, with an overall limit of ρ bits per second. Service Node: When data packets are sent to a service node with a service curve $\beta(t) = \gamma(t-\theta)$, they may experience a waiting time of up to θ before being processed at a rate of γ. An upper bound for delay analysis can be defined as:

$$sup\, t \geq 0 \{ inf\, \tau \geq 0 \{ \tau : A(t) \leq \beta(t + \tau) \} \quad (1)$$

$$\beta 1(t) \otimes \beta 2(t) = inf\, 0 \leq \tau \leq t \{ \beta 1(t - \tau) + \beta 2(\tau) \} \quad (2)$$

When two nodes are linked, the service curves $\beta_1(t) = \gamma_1(t - \theta_1)$ and $\beta_2(t) = \gamma_2(t - \theta_2)$ are combined to form a new service curve $\beta_1(t) \otimes \beta_2(t) = \gamma_3(t - \theta_1 - \theta_2)$, where γ_3 is the minimum of γ_1 and γ_2. In other words, $\gamma_3 = \min \{\gamma_1, \gamma_2\}$.

$$\beta(t) = inf\, 0 \leq \tau \leq t \{ \beta_1(t) \otimes \beta_2(t - \tau_1) \otimes .. \otimes \beta_N(t) \} \quad (3)$$

"N" nodes are linked, the service curves $\beta_1(t) = \gamma_1(t - \theta_1)$, $\beta_2(t) = \gamma_2(t - \theta_2)$, ..., and $\beta_N(t) = \gamma_N(t - \theta_N)$ can be combined to form a new service curve $\beta_1(t) \otimes \beta_2(t) \otimes ... \otimes \beta_N(t) = \gamma_N(t - \theta_1 - \theta_2 - ... - \theta_N)$, where γ_N is the minimum of all individual rates. In other words, $\gamma_N = \min\{\gamma_1, \gamma_2, ..., \gamma_N\}$.

Delay Bound Analysis using SNC

End-users are denoted by I, with service flows fi, each having an arrival curve described by $Ai(t) \leq \rho it + \sigma i$. VNFs introduce delays for data packets due to input/output operations before processing them at a defined rate. The processing behavior of VNFs can be represented by rate-latency service curves, such as $\beta j(t) = \gamma j(t - \theta j)$, where βj(t) is the service curve of the j-th VNF. The equation $\gamma j = \lambda j Rj$ defines a new variable, γj, which represents the capacity of the j-th VNF. Here, λj is the processing rate of the j-th VNF, and Rj is the latency introduced by the j-th VNF.

The service curve analysis focuses on individual queue flows within a Virtual Network Function (VNF). The high and low-priority queue flow totals are represented by $T_j^H(t)$ and T_j^L(tEach flow has a priority denoted by Pij on the j-th VNF, where Pij = 1 indicates high priority and Pij = 0 indicates low priority. Eq. (4) and Eq. (5) model the arrival curves, which describe the incoming data traffic pattern, for the high and low priority queues associated with VNF j. The delay is denoted by $D_i(t)$. According to Proposition 1.3.4 in [XV], high-priority flows have non-pre-emptive priority, ensuring β_j^H(t) service curve with L_{max} packet size. Low-priority flows have β_j^L(t) service curve.

$$T_j^H(t) = \sum_{i=1}^{I} D_i(t)\, P_{ij} \tag{4}$$

$$T_j^L(t) = \sum_{i=1}^{I} D_i(t)\,(1 - P_{ij}) \tag{5}$$

$$\beta_j^H(t) = \beta_j(t) - L_{max} = \gamma_j(t - \theta_j - \tfrac{L_{max}}{\gamma_j}) \tag{6}$$

$$\beta_j^L(t) = \beta_j(t) - T_j^H(t) - L_{max} \tag{7}$$

Within a VNF queue, data processing follows a rate-latency model, as shown in Eq. (6) and Eq. (7). This model highlights the characteristics of individual service flows within the VNF's architecture. According to [IX], a rate-latency server in SNC is defined by its service curve, which guarantees a minimum service rate after an initial latency. The service curve is given by $\gamma(t - \theta)$, where γ is the service rate, t is the time, and θ is the initial latency. Additionally, the server is subject to token-bucket constrained cross traffic, represented by the arrival curve $\rho^c t + \sigma^c$. For non-preempted traffic, assuming pre-emption exists for high-priority traffic, the service curve is given by $(\gamma - \rho^c)(t - \theta - \sigma^c/\gamma)$. This relationship helps in analyzing network performance under varying traffic conditions. In our system, we leverage Eq. (6) and Eq. (7) to determine the guaranteed processing time for each data flow (f_i) within the j-th VNF. These equations enable us to derive the individual service curve for fi. Depending on whether f_i is categorized as high or low priority, its service curve is obtained from either Eq. (8) or Eq. (9). The cross-flow arrival bound is given by $\rho_{ij}^c + \sigma_{ij}^c$ from Eq. (10).

$$\widehat{\beta_{ij}}(t) = (\gamma_j - \rho_{ij}^c)(t - \theta_j - \tfrac{L_{max}}{\gamma_j} - \tfrac{\sigma_{ij}^c}{\gamma_j}) \quad \text{if } P_{ij} = 1 \tag{8}$$

$$\widehat{\beta_{ij}}(t) = (\gamma_j - \sum_{i=1}^{I} \rho_i\, P_{ij} - \rho_{ij}^c)(t - \tfrac{\gamma_j\theta_j + \sum_{i=1}^{I} \sigma_i P_{ij} + L_{max} + \sigma_{ij}^c}{\gamma_j - \sum_{i=1}^{I} \rho_i P_{ij}}) \text{if } P_{ij} = 0 \tag{9}$$

$$\rho_{ij}^c + \sigma_{ij}^c = \begin{cases} T_j^H(t) - D_i(t) & if\ P_{ij} = 1 \\ T_j^L(t) - D_i(t) & if\ P_{ij} = 0 \end{cases} \tag{10}$$

To determine the overall guaranteed processing time for a single data flow in the VNF, we use a rate-latency model detailed in Eq. (8) and Eq. (9). For simplicity, Eq. (11) combines these two equations. Equation (2) outlines how to calculate the overall processing capability (service curve) for a data flow moving through multiple connected network elements. Eq. (12) shows the typical time for a specific data flow (f_i) to go from start to finish, based on calculations from Eq. (13) and Eq. (14). The end-to-end delay bound for data flow f_i is determined using Eq. (1). If the data

transfer rate (service curve rate) exceeds the limit for flow f_i, the end-to-end delay, D_i^{e2e} i exists; otherwise, packet loss occurs, resulting in infiniteD_i^{e2e}.

$$\widehat{\beta_{\iota j}}(t) \triangleq \widehat{\gamma_{\iota j}}\left(t - \widehat{\theta_{\iota j}}\right) \tag{11}$$

$$\gamma_i^{e2e}(t - \theta_i^{e2e}) = \widehat{\beta_{\iota 1}}(t) \otimes \widehat{\beta_{\iota 2}}(t) \ldots \widehat{\beta_{\iota j}}(t) \tag{12}$$

$$\gamma_i^{e2e} = \min j \in [1, J] \{\widehat{\gamma_{\iota j}}\} \tag{13}$$

$$\theta_i^{e2e} = \sum_{J=1}^{J} \widehat{\theta_{\iota j}} \tag{14}$$

$$D_i^{e2e} = \frac{\sigma_i}{\gamma_i^{e2e}} + \theta_i^{e2e} \qquad if\ \gamma_i^{e2e} \geq \rho_i \tag{15}$$

Distribution Function for NFV

Let *S(t)* denote a set of service processes that define the service provided by the network over time t. The arrival process is represented by *A(t)*. The backlog, *B(t)*, and delay, *D(t)* can be described by stochastic variables.

The backlog *B(t)* at time t represents the amount of data that is currently queued in the system, waiting to be processed. The Cumulative Distribution Function (CDF) of the backlog can be used to describe the probability distribution of the backlog, and is given by:

$$F_{B(t)}(b) = P(B(t) \leq b) \tag{16}$$

The CDF of the backlog describes the probability that the backlog at time *t* is less than or equal to a given value *b*. In other words, the CDF represents the probability that the amount of data queued in the system at time *t* is less than or equal to *b*.

The delay *D(t)* represents the duration a data packet spends in the system from arrival to departure. The CDF of the delay quantifies the probability distribution of these waiting times and is expressed as:

$$F_{D(t)}(d) = P(D(t) \leq d) \tag{17}$$

This function describes the probability that a packet's delay is less than or equal to d.

The backlog *B(t)* at time t represents the volume of data currently queued in the system awaiting processing. The Probability Density Function (PDF) of the backlog, which describes the likelihood of the backlog taking on specific values, is expressed as:

$$F_{B(t)}(b) = \frac{d}{dx} P(B(t) \leq b) \tag{18}$$

The delay *D(t)* represents the duration a data packet spends in the system, from arrival to departure. The PDF of the delay, which characterizes the likelihood of different delay times, is expressed as:

$$F_{D(t)}(d) = \frac{d}{dx} P(D(t) \leq d) \tag{19}$$

The node throughput, denoted by *P*, represents the average rate at which packets are successfully delivered over a specific time interval. Here is a clear and concise description of how it can be mathematically described:

$$P = \frac{\sum Number\ of\ packets \times Packet\ Size}{Time\ intervel} \quad (20)$$

$$P = \frac{N(1-\pi_0)f_s D_s}{t} \quad (21)$$

The Packet Delivery Ratio (PDR) is a metric that measures the efficiency of data transmission by evaluating the success rate of packet delivery from the source to the destination. It indicates the proportion of packets that are successfully received compared to the total number of packets sent.

$$PDR = \frac{Number\ of\ packets\ received}{Packets\ Transmitted} \times 100 \quad (22)$$

$$PDR = \frac{(1-\pi_0)f_s}{\lambda t T} \times 100 \quad (23)$$

The expected rate of data arrival at each node is represented by λ. The probability of successful packet transmission by any given station is denoted by fs. The number of nodes is n, the time duration of one slot is T, and the total number of available slots is N. The probability that each node has a packet ready for transmission in the network loop is (1 - π0). Communication efficiency is measured by energy utilization, which considers how well devices manage power across various operational states: transmitting, receiving, idling, and computing. The key performance indicator is the proportion of energy used specifically for successful data transmission between the source and destination nodes.

$$E_u = \frac{E}{n} \quad (24)$$

The energy utilization during data transmission is denoted by E_u. The total energy utilization is represented by E. The number of nodes in the network is denoted by n.

IV. Result Analysis and Discussion

This section explains the implementation of the simulation model in an underwater environment. To ensure a comprehensive assessment of the model's accuracy, simulation experiments are conducted in the OMNeT++ environment. This professional approach guarantees a thorough evaluation of the model's performance and reliability [XX]. The INET framework is utilized in the OMNeT++ simulation environment to simulate communication networks. As an open-source tool, INET supports researchers and developers in analyzing and enhancing network performance effectively. The framework is structured around modular communication via message passing, where components represent agents and network protocols. This enables flexible assembly into hosts, routers, switches, and various networking tools [XXIX]. To demonstrate the deployment of VNFs, two sample VNFs are employed: a firewall and a Network Address Translation (NAT) service. Each VNF utilizes two threads, ensuring efficient execution and management of network functions.

These threads utilize the DPDK interface [VI] to fetch packets from the Acoustic Modem and route them to appropriate queues based on the packets' five-tuple information (source IP, destination IP, source port, destination port, and protocol). The packets are retrieved from the queues according to the scheduling policy, processed, and then seamlessly forwarded to the next VNF instance or another

Acoustic Modem. Each thread is dedicated to a specific CPU core to ensure optimal performance. A DPDK-based packet generator is used to accurately measure packet delay in traffic transmission. In our experiments, the packet lengths are adjusted to 800 bytes. To evaluate the performance of our SNC analysis, we set up an experiment with three data streams: a main data flow (f1) and two additional flows (f2 and f3) that could potentially disrupt it. All three flows are modeled using TBFs.

Table 1 : The Parameters of Arrival and Service Curves

Flow Arrival Curve		
Parameters	***Rate***	***Max Burst***
Tf (f1)	700 kbps	18 kb
Cf 1 (f2)	3100 kbps	88 kb
Cf (f3)	1500 kbps	26 kb
Service Curve		
Parameters	***Rate***	***Latency***
(VNF -1) Firewall	12100 kbps	97 µs
(VNF-2) Network Address Translation	32280 kbps	60 µs
Tf - Through flow, Cf - Cross flow		

VNF performance is assessed by data throughput and latency. Data throughput, measured in bits per second, determines the maximum processing rate before packet loss. Latency, measured in microseconds, represents the time delay introduced by the VNF [XXIV]. A firewall and a NAT, with respective throughputs of 12,100 kbps and 32,280 kbps, and latencies of 97 and 60 microseconds, were analyzed using TBF parameters for different flows. Two scenarios simulated different priority configurations for flows f1, f2, and f3 in a single firewall and then with a NAT added. The longest calculated delays were 4,561.13 microseconds in the first scenario and 6,242.55 microseconds in the second, providing valuable insights into system performance under various conditions.

The Transport layer's functionality was evaluated using discrete-event simulations. The simulation consisted of 50 nodes, each representing an underwater seaweed meadow, uniformly spaced and equipped with underwater sensor nodes that collect data. The node setup parameters are outlined in Table 2. These meadows are submerged at depths ranging from 45 to 55 meters.

The performance of these nodes is critical for the effective management of the Transport layer, which regulates packet flow and size allocation. This is essential for ensuring reliable underwater communication. Insufficient evaluation of packet flow can increase the risk of data loss, potentially impacting other network layers due to the interconnected nature of wireless architectures. To maintain data integrity, optimize network efficiency, and minimize data loss in wireless networks, a comprehensive assessment of node performance is indispensable.

Table 2: Parameters of Simulation

Parameter	**Value**
Number of Nodes	50
Antenna type	Omni-directional antenna
Packet size	2100 bytes

Traffic rate	110-1600 Kbps
Simulation time (s)	2000
Communication mode	Half-duplex communication
Channel	Underwater acoustic channel
Transmission type	Bit rate
Range	45-55 m
Node service queue	Delay-Tolerant Queue
buffer queue	M/G/1

The CDF of packet delays for flow f1, as shown in Fig. 3, indicates that the observed maximum delay for any packet did not surpass the predetermined threshold. However, in practice, packet delays frequently exceed these thresholds, resulting in discrepancies between observed and expected delays. Scenario One requires a highly unlikely event: flows f1 and f2 simultaneously producing maximum bursts. This is necessary to bridge the gap between the actual and theoretical delay constraints, making it a loose bound. In Scenario Two, achieving the maximum predicted delay also necessitates an improbable scenario: concurrent peak traffic for all three flows. Consequently, the likelihood of encountering the maximum delay in Scenario Two is lower.

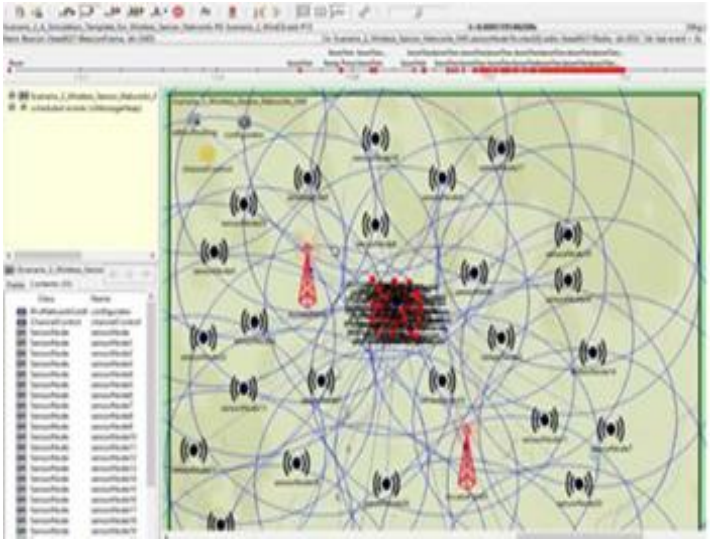

Fig. 3. Simulation node setup for NFV in an underwater environment

In an underwater environment, packets are transmitted as acoustic signals between randomly deployed nodes spaced 50-100 meters apart. Packet transmissions occur only during scheduled times, determined by the cluster head, and communicated through beacon frames to nodes within a 1600-meter range. The cluster head is selected based on its high energy level. Initially, one node serves as the cluster head for transmitting signals to a buoy. Fig. 3 illustrates the simulation node setup for this underwater environment. When a node's energy level drops to 50%, it enters sleep mode, transferring signal responsibility to other groups. The performance of the simulation model and the SNC model was compared in terms of throughput, packet delivery ratio, and energy utilization of NFV using SNC. Scenarios 1 and 2 were used

to analyze delay variations using CDF probability, and the results were compared and analyzed in Fig. 4 and Fig. 5.

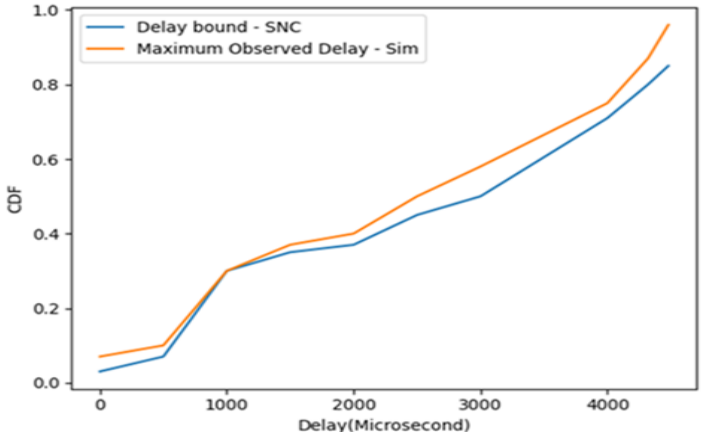

Fig. 4. Comparison of Cumulative Distribution Function (CDF) with SNC-derived Delay Bounds for Scenario 1.

The comparative analysis of delay and Cumulative Distribution Function (CDF) is presented in Fig 4, where the blue line represents the SNC model and the orange line represents the simulation model. The x-axis indicates the delay bounds (µs) derived from Eq. (17), and the y-axis represents the CDF. The analysis shows that when the CDF is 0.09, both models exhibit a delay of 0 µs, and at a CDF of 0.4, both models have a delay of 1100 µs. However, as the CDF increases, the SNC model tends to produce lower delays, with a delay of 4900 µs at a CDF of 0.81, compared to the simulation model, which reaches a delay of 4900 µs at a CDF of 0.94. Overall, the SNC model shows a slightly better performance, with a difference ranging from 3% to 6% compared to the simulation model.

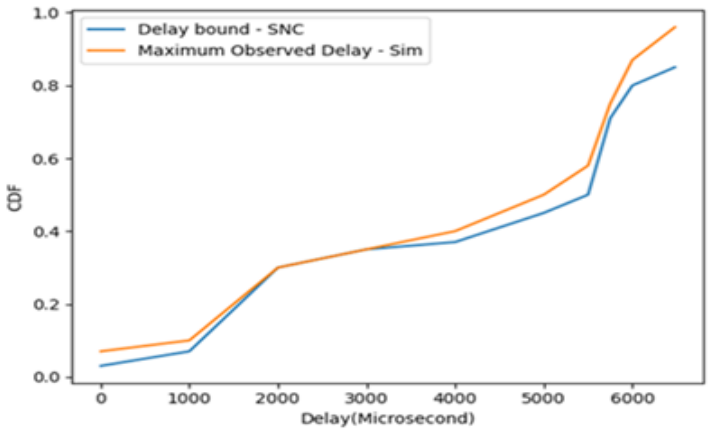

Fig. 5. Comparison of Cumulative Distribution Function (CDF) with SNC-derived Delay Bounds for Scenario 2

Fig. 5 compares the delay bounds and CDFs of the simulation model (orange line) and the SNC model (blue line). The x-axis represents delay bounds in microseconds

(µs), and the y-axis represents the CDF. At a CDF of 0.09, both models exhibit a delay of 0 µs. At a CDF of 0.4, both models show a delay of 2100 µs. The delay increases linearly, reaching 3300 µs at a CDF of 0.39. However, at a CDF of 0.97, the simulation model exhibits a delay of 6700 µs, while the SNC model shows a delay of 6700 µs at a CDF of 0.87. This comparison demonstrates that the SNC model generally achieves lower delays than the simulation model, with an improvement ranging from 1% to 4%.

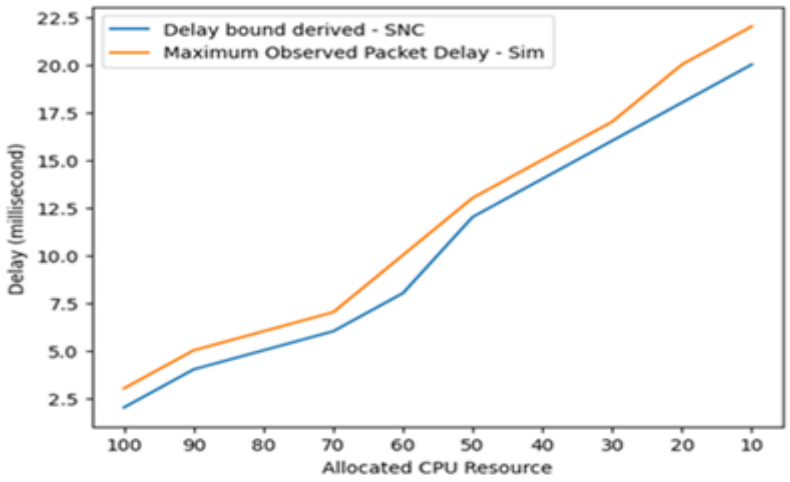

Fig. 6. Comparison of the maximum delays observed in packet transmissions during the experiments. This comparison was done by changing the amount of CPU resources allocated to the VNF.

Fig. 6 compares allocated CPU resources and delay for the SNC model (blue line) and the simulation model (orange line). The x-axis represents allocated CPU resources, and the y-axis indicates delay in milliseconds (ms). At 100 CPU resources, both models exhibit a delay of 2.8 ms. As CPU resources decrease, the delay increases. However, the SNC model consistently demonstrates lower delays than the simulation model. For example, at 12 CPU resources, the simulation model shows a delay of 20 ms, while the SNC model achieves a delay of 19.9 ms. This comparison indicates that the SNC model generally produces lower delays compared to the simulation model, with a difference ranging from 3% to 5%.

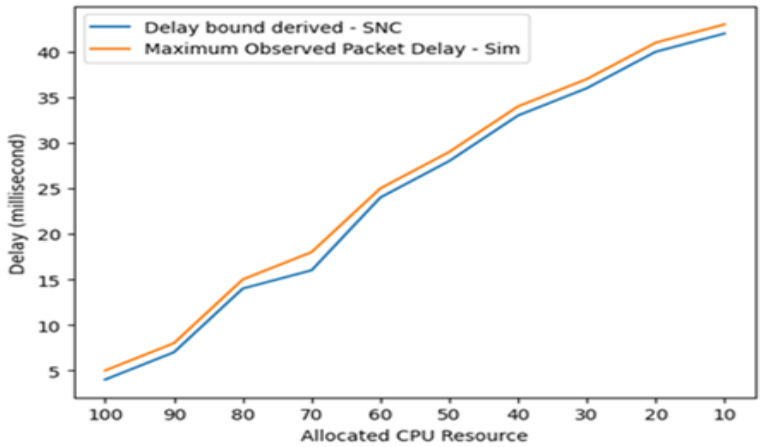

Fig. 7. Comparison of the maximum delays observed in packet transmissions during the experiments. This comparison was done by changing the amount of CPU resources allocated to the VNF.

Fig. 7 compares allocated CPU resources and delay for the SNC model (blue line) and the simulation model (orange line). The x-axis represents allocated CPU resources, and the y-axis indicates delay in milliseconds (ms). At 100 CPU resources, the SNC model exhibits a delay of 2 ms, which is lower than the simulation model's delay of 4 ms. When CPU resources are reduced to 9, the SNC model shows a delay of 42 ms, while the simulation model experiences a higher delay of 42 ms. This comparison demonstrates that the SNC model generally produces lower delays compared to the simulation model, with a difference ranging from 1% to 3%.

This research study investigates the impact of CPU resource allocation on VNFs, as illustrated in Fig. 6 and Fig. 7. A linear decrease in CPU allocation results in a more rapid increase in the derived delay bound, emphasizing the importance of CPU resources for VNF performance optimization. The derived delay bound is inversely related to the VNF rate, as described in Eq. (15). This means that with more processing power allocated to the firewall, the actual packet delay approaches the predicted maximum delay. Even at a 10% CPU allocation (4200 kbps), the firewall's rate is lower than the combined rates of flows f1 and f3. This can contribute to the observed behavior, as the conditions outlined in Eq. (15) are not met, making the SNC theory inapplicable. Experimental results demonstrate packet loss in this scenario, implying infinite and unobservable packet delay.

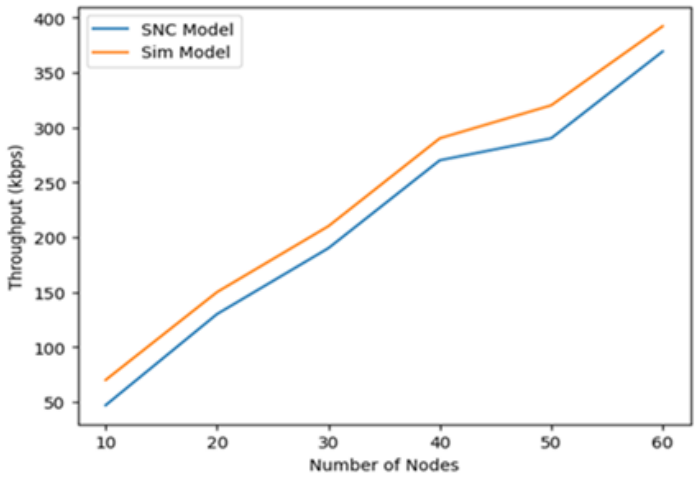

Fig. 8. Throughput vs Number of Nodes

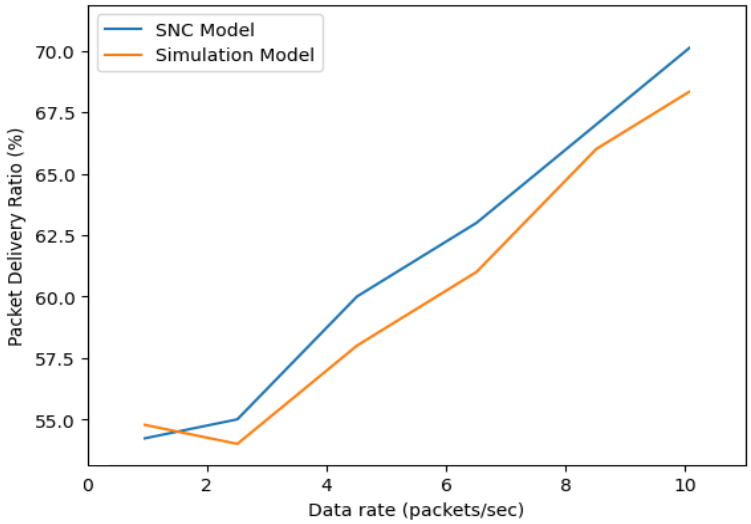

Fig. 9. Packet Delivery Ratio vs Data rate

A simulation and SNC-based analytical model were developed for an underwater scenario involving 50 nodes with half-duplex communication. Half-duplex communication was chosen to prevent data loss and energy waste caused by collisions, which can occur with full-duplex communication. The total amount of acoustic signals transmitted within a specific timeframe was analyzed in Fig. 8. Both the simulation model (orange line) and SNC model (blue line) demonstrate a linear increase in throughput as the number of nodes grows. Both models perform VNF functionalities and monitor successful node connectivity using data link layer protocols. The simulation model achieved a minimum throughput of 281 bytes among 10 nodes over 9,61,000 milliseconds of execution, while the SNC model reached 346 bytes during the same period. The maximum throughput was 371 kbps for the simulation model and 397 kbps for the SNC model, representing a significant

improvement of 4% to 7% in the SNC-based model. A comparative analysis reveals that the SNC model for NFV outperforms the simulation-based NFV model in traffic management aspects. The similarity index between the SNC model and simulation model was also evaluated using discrete event simulation to assess its accuracy.

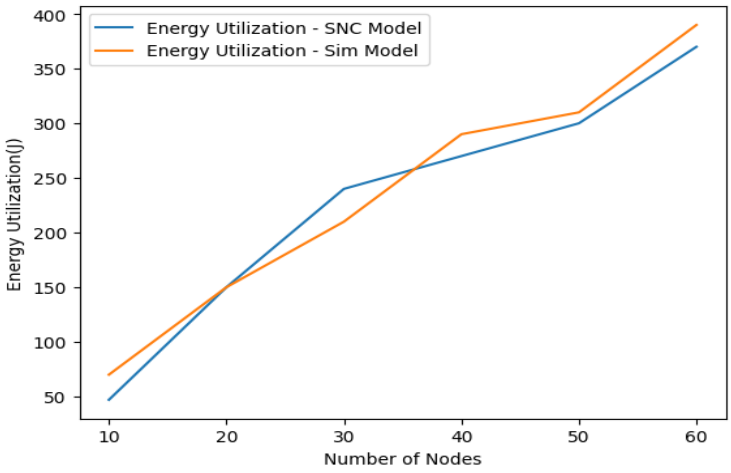

Fig. 10. Energy Utilization vs Number of Nodes

Analyzing the packet delivery ratio (PDR) for underwater environments using NFV is essential for further research. Fig. 9 compares the PDR between nodes using the SNC model (blue line) and simulation model (orange line) for 60 sensor nodes with half-duplex communication and time division multiplexing. Packet rates were increased from 0 to 10 per second. Initially, the SNC model achieved a 52% PDR for 1 packet per second, while the simulation model obtained a 54% PDR. As the number of packets increased, the SNC model's PDR gradually improved. The SNC model outperformed the simulation model in terms of PDR for NFV functionality analysis. For 10 packets per second, the SNC model achieved a 69% PDR compared to the simulation model's 68%, representing a significant improvement of 5% to 7% in modeling NFV using SNC over the simulation model.

Fig. 10 compares energy utilization between nodes using the SNC model (blue line) and the simulation model (orange line). As the number of nodes increases, energy utilization rises in the simulation model. However, the SNC model demonstrates strong performance, with energy utilization gradually decreasing as the number of nodes grows. A correlation between the SNC and simulation models is observed at 21 and 36 nodes. The SNC model outperforms the simulation model in NFV functionality analysis, achieving lower energy utilization and representing a significant improvement of 5% to 7% when using the SNC approach. Additionally, the VNF instance rate correlates with resource allocation, as shown in Fig. 11. The orange line represents the VNF firewall, and the blue line represents the VNF NAT. As allocated CPU resources increase, the VNF rate also increases, highlighting a significant difference between processing rate and allocated CPU resources. Specifically, when 82% of the CPU resource is allocated to the underwater sensor node, the VNF rate increases to 37kpps.

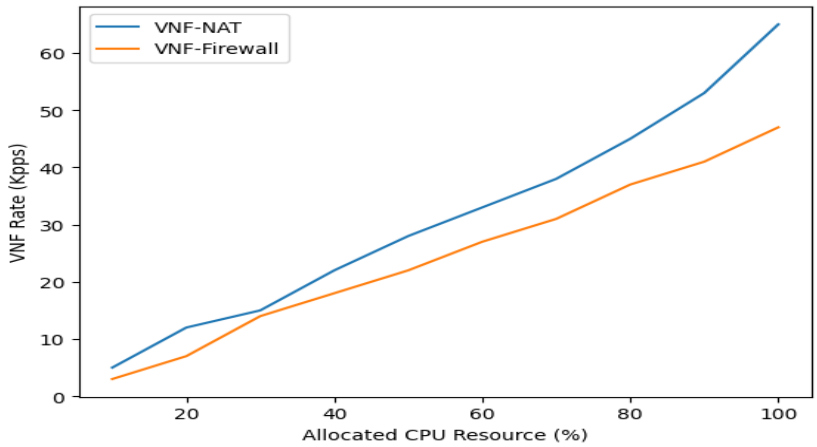

Figure 11. Impact of allocated CPU resources on VNF processing rate

Comparative studies of throughput, delay, and backlog in the SNC model using NFV demonstrate several advantages. NFV enables load balancing across multiple VNFs, contributing to lower delay bounds during periods of high traffic. It also aids in managing high traffic volumes, reducing backlog, and improving energy efficiency. As the number of nodes increases, the SNC model demonstrates lower energy utilization compared to the simulation model, enhancing reliability and reducing packet loss, which leads to an improved packet delivery ratio. The SNC-based approach is used to evaluate the performance of NFV-based firewalls and data collection systems under various traffic conditions and scenarios.

V. Conclusion

For effective long-term monitoring, extending the lifecycle of the network hardware that is in place for the communication and reduction of the power consumption involved plays a crucial role. In addition to this UWSN also demands rapid deployments. To achieve these demands of UWSN adoption of NFV in UWSN becomes critical. Specifically, in this research, the SNC-based mathematical model for NFV of UWSN has been created and its performance concerning maximum delays experienced by data flows across a series of VNFs has been analyzed. The model accounts for priority levels assigned to individual VNFs while enabling the sharing of VNF resources. To analyze the performance of the proposed model, the appropriate analytical bounds have been derived for performance metrics such as delay, throughput, and energy utilization and the same has been compared with the simulation results. The evaluation results show a close correlation between the simulation results and the analytical results. In the future, this work will be extended to the transport layer NFV functionalities with feedback loop unit operations and optimized packet management in UAWSN environments.

Conflict of Interest:

There was no relevant conflict of interest regarding this paper.

References

I. Awan, Khalid Mahmood, et al. "Underwater wireless sensor networks: A review of recent issues and challenges." Wireless Communications and Mobile Computing 2019.1 (2019): 6470359, 10.1155/2019/6470359.

II. Bennouri, Hajar, and Amine Berqia. "U-NewReno transmission control protocol to improve TCP performance in Underwater Wireless Sensors Networks." Journal of King Saud University-Computer and Information Sciences 34.8 (2022): 5746-5758, 10.1016/j.jksuci.2021.08.006.

III. Bhamare, Deval, et al. "Optimal virtual network function placement in multi-cloud service function chaining architecture." Computer Communications 102 (2017): 1-16, 10.1016/j.comcom.2017.02.011.

IV Bari, Faizul, et al. "Orchestrating virtualized network functions." IEEE Transactions on Network and Service Management 13.4 (2016): 725-739, 10.1109/TNSM.2016.2569020.

V. Coutinho, Rodolfo WL, et al. "Underwater wireless sensor networks: A new challenge for topology control–based systems." ACM Computing Surveys (CSUR) 51.1 (2018): 1-36. 10.1145/3154834.

VI. Data Plane Development Kit, Jan. 2021, [online] Available: https://www.dpdk.org/.

VII. Duan, Qiang. "Modeling and performance analysis for service function chaining in the SDN/NFV architecture." 2018 4th IEEE Conference on Network Softwarization and Workshops (NetSoft). IEEE, 2018.. IEEE, 10.1109/NETSOFT.2018.8460068.

VIII. Fattah, Salmah, et al. "A survey on underwater wireless sensor networks: Requirements, taxonomy, recent advances, and open research challenges." Sensors 20.18 (2020): 5393, 10.3390/s20185393.

IX. Fidler, Markus. "Survey of deterministic and stochastic service curve models in the network calculus." IEEE Communications surveys & tutorials 12.1 (2010): 59-86, 10.1109/SURV.2010.020110.00019.

X. Gouareb, Racha, Vasilis Friderikos, and Abdol-Hamid Aghvami. "Virtual network functions routing and placement for edge cloud latency minimization." IEEE Journal on Selected Areas in Communications 36.10 (2018): 2346-2357. 10.1109/JSAC.2018.2869955.

XI. Haque, Khandaker Foysal, K. Habibul Kabir, and Ahmed Abdelgawad. "Advancement of routing protocols and applications of underwater wireless sensor network (UWSN) — A survey." Journal of Sensor and Actuator Networks 9.2 (2020): 19. 10.3390/jsan9020019.

XII. Hassan, Mohamed Khalafalla, et al. "A Short Review on the Dynamic Slice Management in Software-Defined Network Virtualization." Engineering, Technology & Applied Science Research 13.6 (2023): 12074-12079, 10.48084/etasr.6394.

XIII. Huang, Xiangdang, Shijie Sun, and Qiuling Yang. "Data uploading strategy for underwater wireless sensor networks." Sensors 19.23 (2019): 5265. 10.3390/s19235265.

XIV. Huh, Jun-Ho. "Reliable user datagram protocol as a solution to latencies in network games." Electronics 7.11 (2018): 295, 10.3390/electronics7110295.

XV. Le Boudec, Jean-Yves, and Patrick Thiran, eds. Network calculus: a theory of deterministic queuing systems for the internet. Berlin, Heidelberg: Springer Berlin Heidelberg, 2001, https://doi.org/10.1007/3-540-45318-0.

XVI. Liang Y, Ji-Liu Z. et al. "A study of transmission control protocol for satellite network". In2009 5th International Conference on Wireless Communications, Networking and Mobile Computing (2009), https://doi.org/10.1109/WICOM.2009.5303023.

XVII. Miao, Wang, et al. "Performance modelling and analysis of software-defined networking under bursty multimedia traffic." ACM Transactions on Multimedia Computing, Communications, and Applications (TOMM) 12.5s (2016): 1-19, https://doi.org/10.1145/2983637.

XVIII. Miao, Wang, et al. "Stochastic performance analysis of network function virtualization in future internet." IEEE Journal on Selected Areas in Communications 37.3 (2019): 613-626, 10.1109/JSAC.2019.2894304.

XIX. Mijumbi, Rashid, et al. "Network function virtualization: State-of-the-art and research challenges." IEEE Communications surveys & tutorials 18.1 (2015): 236-262. 10.1109/COMST.2015.2477041.

XX. Omnet++ User Guide. In Version 5.4.1, Budapest, Hungary, 2016.

XXI. Qu, Long, et al. "A reliability-aware network service chain provisioning with delay guarantees in NFV-enabled enterprise datacenter networks." IEEE Transactions on Network and Service Management 14.3 (2017): 554-568. 10.1109/TNSM.2017.2723090.

XXII. Saravanan, M., et al. "Medium Access Control layer protocol design based on stochastic network calculus for underwater wireless communication in open-ocean fish farming." International Journal of Communication Systems 35.8 (2022): e5118, 10.1002/dac.5118.

XXIII. Saravanan, M., Sukumaran, R. et al. "Underwater Cross Layer Protocol Design for Data Link Layer: Stochastic Network Calculus". International Journal of Computing, (2023), 367-380, 10.47839/ijc.22.3.3233.

XXIV. Stiliadis, Dimitrios, and Anujan Varma. "Latency-rate servers: a general model for analysis of traffic scheduling algorithms." IEEE/ACM Transactions on networking 6.5 (1998): 611-624, 10.1109/90.731196.

XXV. Stojanovic M. et al. “Acoustic (underwater) communications”. Wiley Encyclopedia of Telecommunications. (2003). 10.1002/0471219282.eot110.

XXVI. Wang, Zenan, Jiao Zhang, and Tao Huang. "Determining delay bounds for a chain of virtual network functions using network calculus." IEEE Communications Letters 25.8 (2021): 2550-2553. 10.1109/lcomm.2021.3065147.

XXVII. Yang, Guang, Lie Dai, and Zhiqiang Wei. "Challenges, threats, security issues and new trends of underwater wireless sensor networks." Sensors 18.11 (2018): 3907. 10.3390/s18113907.

XXVIII. Yi, Bo, et al. "A comprehensive survey of network function virtualization." Computer Networks 133 (2018): 212-262, 10.1016/j.comnet.2018.01.021.

XXIX. https://inet.omnetpp.org/docs/users-guide/